

Short Communication

Effect of Silicon Content on Corrosion Resistance of a Cold Rolled Non-Oriented Silicon Steel

Yuan Lin^{1,2,*}, Hongxia Wang^{1,*}, Jin Xiang³, Hui Wei¹, Zilong Zhao^{4,*}, Wenkang Zhang², Yide Wang^{1,2}

¹ College of Materials Science and Engineering, Taiyuan University of Technology, Taiyuan 030024, China

² Technical Center, Taiyuan Iron & Steel (Group) Co., Ltd., Taiyuan 030003, China.

³ Department of Mechanics, Jinzhong University, Jinzhong, 030600, Shanxi, China

⁴ School of Chemical Engineering and Technology, Sun Yat-sen University, Zhuhai 519082, China

*E-mail: linyuan@tisco.com.cn; wanghxia1217@163.com; zhaozlong@mail.sysu.edu.cn

Received: 3 December 2021 / Accepted: 24 January 2022 / Published: 2 February 2022

Non-oriented silicon steel is a critical functional material for various types of motor iron cores. When the motor was rotating at high speed in the rainy season, the iron core materials rusted easily. In this paper, the corrosion resistance of low silicon, medium silicon and high silicon non-oriented silicon steel in wet and hot environments was studied. The phase of three materials was tested by XRD, the microstructure and surface morphology before and after corrosion of silicon steel were studied and compared by three-dimensional ultradepth-of-field microscopy. The morphology and composition after corrosion of silicon steel were measured by scanning electron microscope and composition analysis spectrum. The corrosion mechanism of cold rolled non-oriented silicon steel with different silicon contents in wet and hot extreme environments was discussed.

Keywords: non-oriented silicon steel, Si content, corrosion resistance, oxidization film

1. INTRODUCTION

Non-oriented silicon steel is an indispensable soft magnetic material in the power, electronics and military industries. It is mainly used in the manufacture of motor iron cores[1-3]. Due to the long production process and complex manufacturing process, its manufacturing technology and product quality are important symbols to measure the production and scientific and technological development level of a country's special steel[4]. According to different magnetic properties, non-oriented silicon steel is generally divided into three categories: high grade, high magnetic induction and medium and low grade. In general, the higher the Si content is, the higher the brand, the better the magnetic properties, and the lower the energy consumption of the manufactured motor[5]. Many studies have

been carried out on the factors affecting the magnetic properties in the manufacturing process of non-oriented silicon steel, such as composition, texture, grain size, thickness and stress. However, the effect of surface quality on the magnetic properties of silicon steel sheets has not been deeply studied, especially corrosion[6]. The coating will be applied after annealing in the large-scale production of non-oriented silicon steel to ensure insulation and reduce corrosion. When the climate is hot and humid, especially in the rainy season, the surface of silicon steel sheets easily rust during storage or processing, resulting in product magnetic properties, which not only affects the motor efficiency[7], but also damages the user's mold during punching and reduces the service life[8]. Therefore, it is of great significance to study the corrosion resistance of non-oriented silicon steel in a damp heat coupling environment.

By simulating a humid environment, this paper studies the changes of phase, microstructure, surface morphology and composition of non-oriented silicon steel sheets with different silicon contents before and after corrosion, to provide technical support for the corrosion problems encountered by users in the process of using and processing silicon steel sheets.

2. EXPERIMENTAL PROCEDURE

The raw materials are high grade, high magnetic induction and low grade cold rolled non-oriented silicon steel finished plates with a thickness of 0.50 mm produced by Taiyuan Iron & Steel (Group) Co., Ltd., China. The Si content of high grade non-oriented silicon steel is generally above 2.0% with both lower iron loss and lower magnetic induction. The Si content of high magnetic induction non-oriented silicon steel is 1.6%~2.0% with higher magnetic induction, but the iron loss is worse than high grade silicon steel. The Si content of medium and low grade is below 1.6%, the iron loss is worst and the magnetic induction is between high grade and high magnetic induction silicon steel. The manufacturing process is: smelting → hot rolling → (normalization) → cold rolling (0.50 mm) → annealing and coating. Among them, high grade and high magnetic induction non-oriented silicon steel are normalized and pickling (after shot blasting), while low grade non-oriented silicon steel is not normalized and directly cold rolled after hot rolling. The main compositions are shown in Table 1. 1# is low-grade non-oriented silicon steel, 2# is high induction non-oriented silicon steel and 3# is high-grade non-oriented silicon steel. The Si and Al contents of sample 3# are the highest among the three samples.

Table 1. Chemical compositions of non-oriented silicon steel, wt.%

| Sample | Si | Al | Mn | S | N | C | Fe |
|--------|------|------|------|--------|--------|--------|-----|
| 1# | 1.08 | 0.25 | 0.15 | 0.0020 | 0.0020 | 0.0030 | Bal |
| 2# | 1.75 | 0.32 | 0.56 | 0.0015 | 0.0020 | 0.0030 | Bal |
| 3# | 3.27 | 0.94 | 0.15 | 0.0010 | 0.0020 | 0.0020 | Bal |

The microstructures were examined by using an optical microscope (OM , LEICA DVM6) and a scanning electron microscope (SEM, JSM-7800F, JEOL, Japan) equipped with an Oxford electron

backscattered diffraction system. Phase analysis was carried out on an XPERT-PRO X-ray diffraction (XRD) system. The electrochemical properties of the obtained substrate surface were determined in 3.5 wt% NaCl aqueous 60 °C solution and subsequently placed in an ultrasonic bath (KQ-300VDE, Kongshan, 45 kHz) at 100% ultrasound power. An electrochemical workstation (GAMRY, 25207) was used, which was equipped with a standard three-electrode system with an Ag/AgCl reference electrode, and the counter electrode was a platinum electrode. The working electrode was arranged in a homemade holder of Teflon, which had a circular window with an area of 1 cm² exposed to the electrolyte. The potentiodynamic polarization curves were measured from -400 to +800 mV vs OCP at a scan rate of 1 mV s⁻¹.

3. RESULTS AND DISCUSSION

Fig. 1 is an OM diagram of non-oriented silicon steel with different silicon contents before corrosion. There are many white bands in the left figure of high grade and high magnetic induction non-oriented silicon steel, which means that the coating is not even as the silicon content increases.

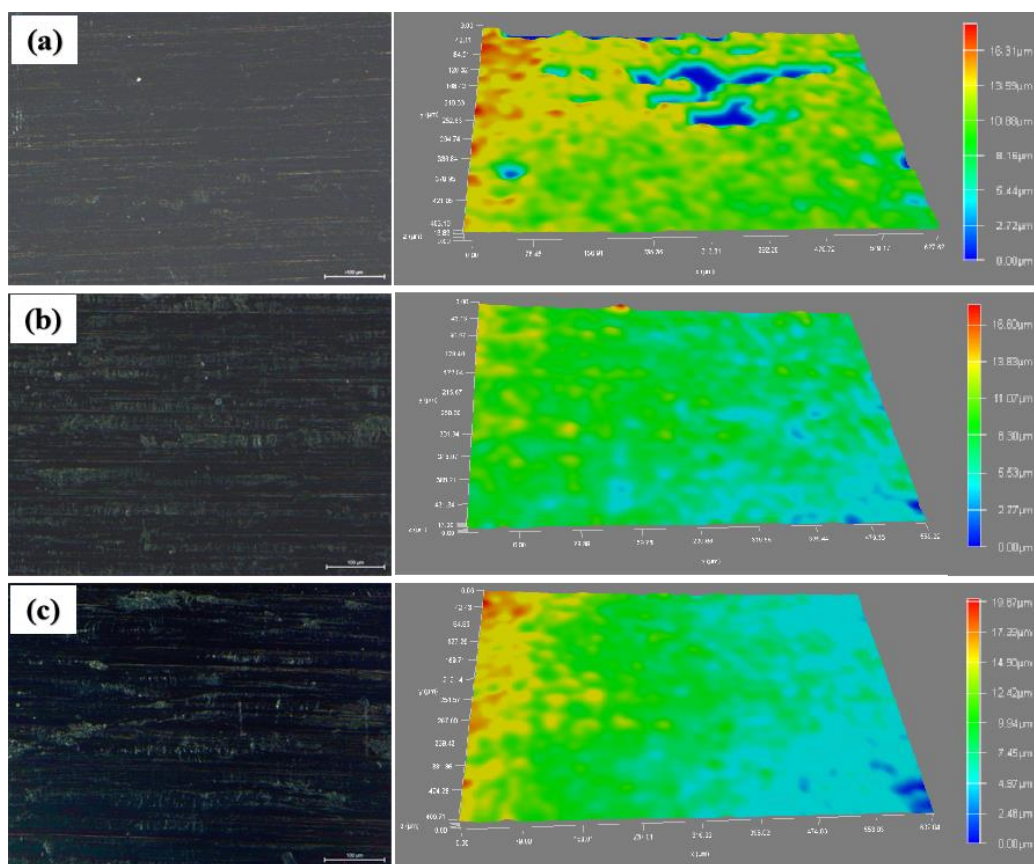


Figure 1. OM images of electrical steel before corrosion (a) 1# and (b) 2# and (c) 3#

When the Si content is increases, the bulky columnar grain ratio in cast slabs also increases, which can lead to inhomogeneous grain sizes and detrimental surface[9-11]. In addition, compared with the low grade hot-rolled plate production process, the high grade and high magnetic induction

hot-rolled plates should be normalized and pickled (after shot blasting) to raise the magnetic properties and remove the scale[12]. The process of shot blasting and pickling will increase the hot-rolled plate surface roughness. For these reasons, the substrate roughness of cold-rolled non-oriented silicon steel increases with increasing Si content due to the heredity of the slab microstructure and hot-rolled plate surface state, which results in the surface coating being uneven.

Fig. 2 shows the XRD pattern of the three silicon steel sheets. For each XRD pattern of the silicon steel sheet with different Si contents, one strong peak and three weak peaks at approximately $2\theta = 44.6^\circ$, 64.9° , 82.1° and 98° were detected, which correspond to the (110), (200), (211) and (220) crystal planes of cubic α -Fe using Jade software. There is no obvious change in the diffraction peaks except for the intensities. This shows that the phase categories of non-oriented silicon steel are not influenced by the Si content.

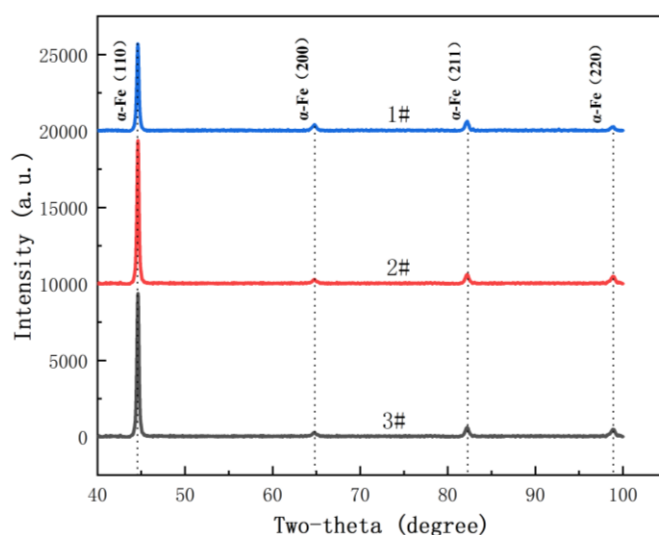


Figure 2. The XRD patterns of non-oriented silicon steel with different Si contents.

Fig. 3 shows potentiodynamic polarization curves of non-oriented silicon steel. It can be seen from the figure that high-grade non-oriented silicon steel has the optimal self-corrosion potential and corrosion current. Combined with Table 2, the self-corrosion potential is -0.546 . The self-corrosion potentials of high magnetic induction and low grade non-oriented silicon steel are -0.575 and -0.595 respectively. Sample 3# has the lowest corrosion current, which is 6×10^{-7} , which indicates that Sample 3# has strong corrosion resistance[13-14]. The above results show that non-oriented silicon steel has good self-corrosion potential and maintains high corrosion resistance in the extreme environment of wet thermal coupling. It has been reported that an increase in silicon and aluminum is conducive to improving the corrosion resistance of non-oriented silicon steel. Cold-rolled non-oriented silicon steel inevitably oxidizes during continuous annealing even in a protective atmosphere [15]. When the Si or Al alloy content is increasing, the substrate surface roughness before annealing is higher which oxidizes more easily, and a dense oxidization film is formed on the surface, which prevents the surface from been further oxidized..

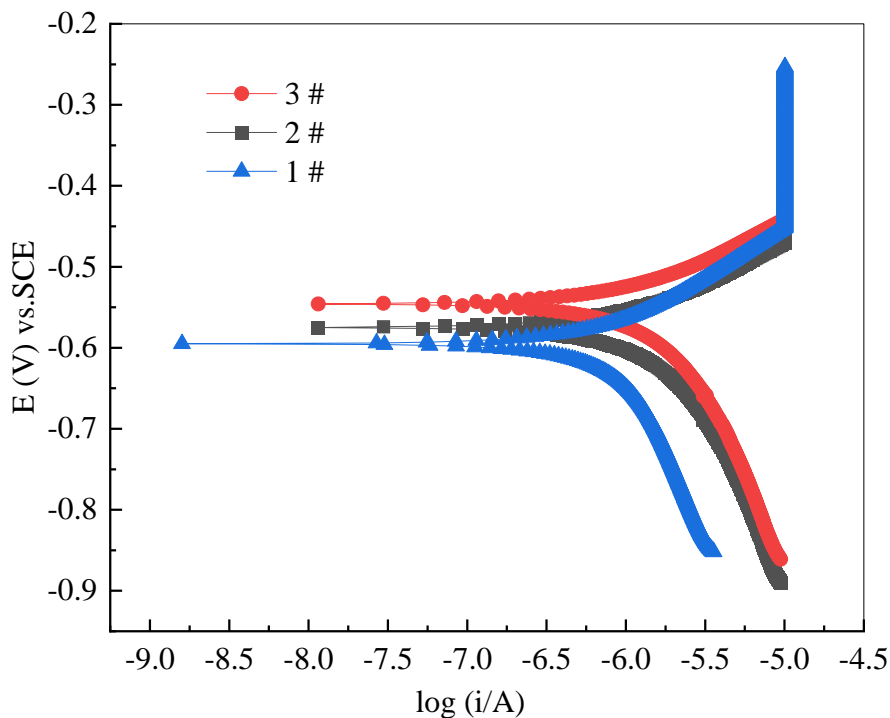


Figure 3. Potentiodynamic polarization curves of non-oriented silicon steel in a 3.5 wt% NaCl aqueous 60 °C solution and subsequently placed in an ultrasonic bath at 100% ultrasound power.

Table 2. Electrochemical and corrosion parameters of non-oriented silicon steel in Figure 3.

| Sample | E _{corr} (VSCE) | i _{corr} |
|--------|--------------------------|-----------------------|
| 1# | -0.595 | 6.5×10 ⁻⁷ |
| 2# | -0.575 | 6.25×10 ⁻⁷ |
| 3# | -0.546 | 6×10 ⁻⁷ |

After the non-oriented silicon steel sheet is corroded, it can be observed from Figure 4 that there are obvious corrosion pits on the surface of the low grade non-oriented silicon steel, indicating that local corrosion occurs. The surface of high magnetic induction and high grade non oriented silicon steel is dominated by whitebands, indicating that the roughness is higher, which oxidizes easily and forms a dense oxidization film that prevents further oxidation. However, some corrosion points also appear on the surface layer of high grade and high magnetic induction non-oriented silicon steel in humid and high temperature atmospheric conditions.

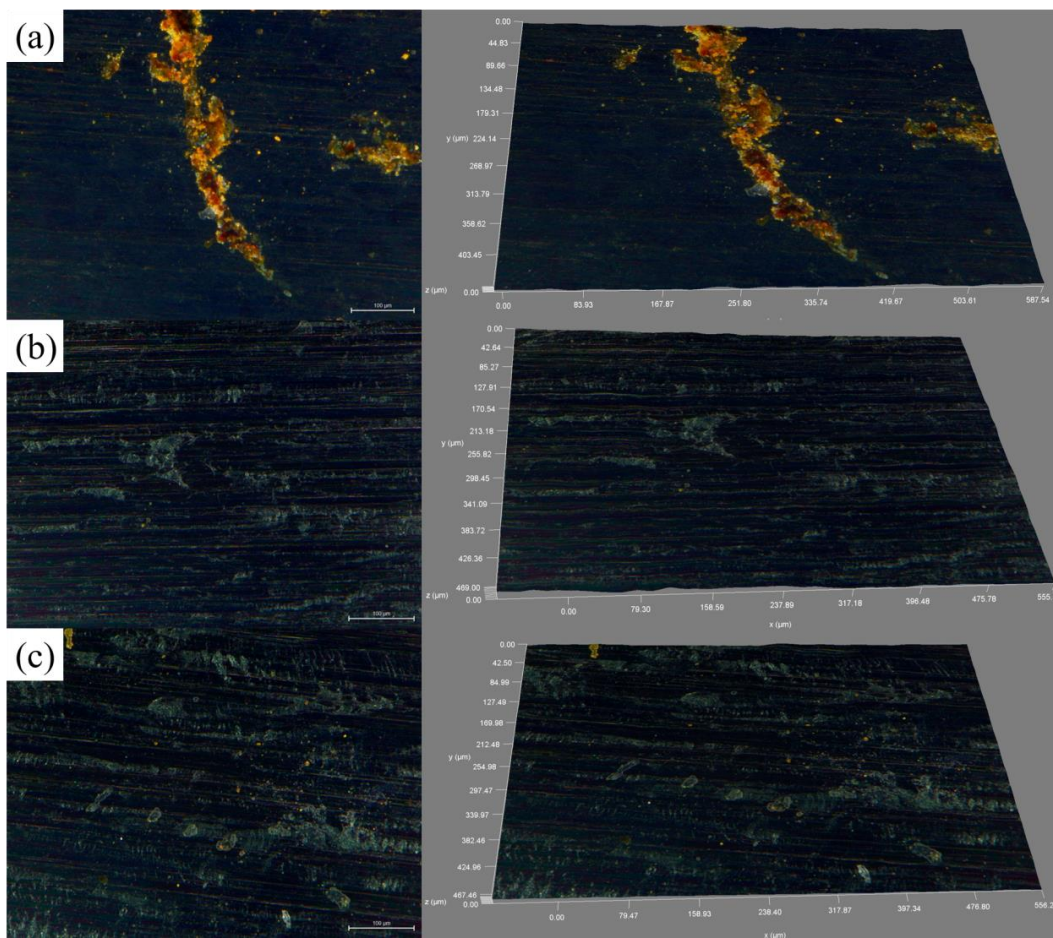


Figure 4. OM images of corroded non-oriented steel after corrosion (a) 1# and (b) 2# and (c) 3#

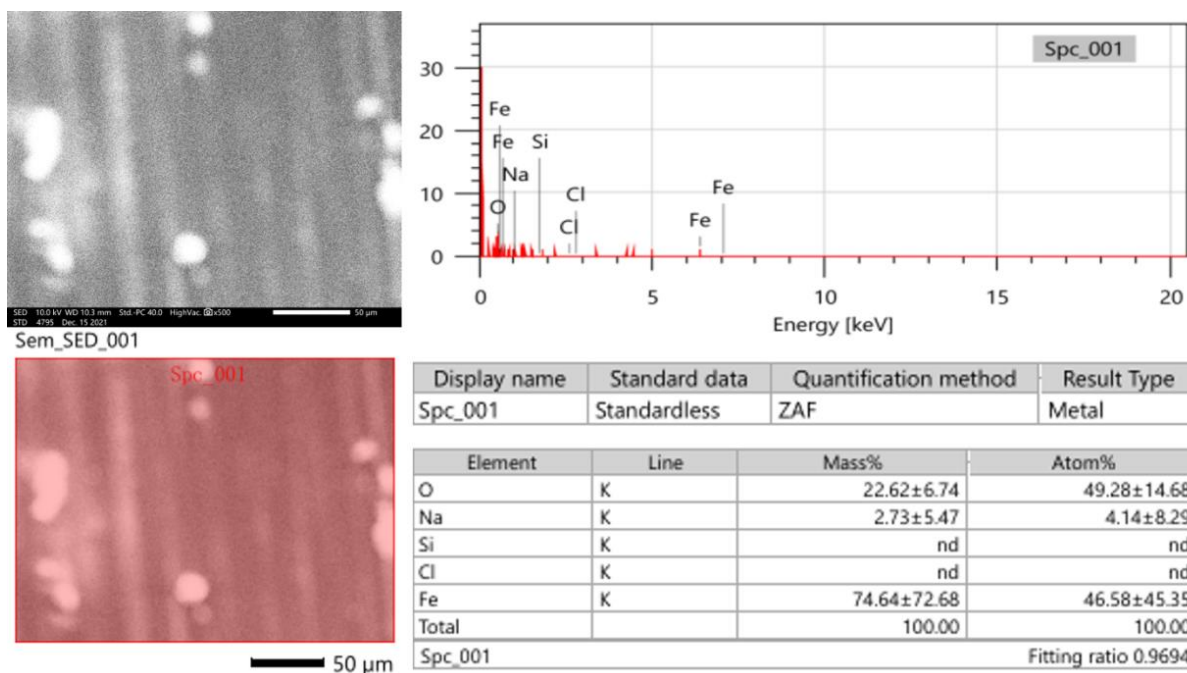


Figure 5. SEM images and EDS of 1# low-grade non-oriented silicon steel after corrosion

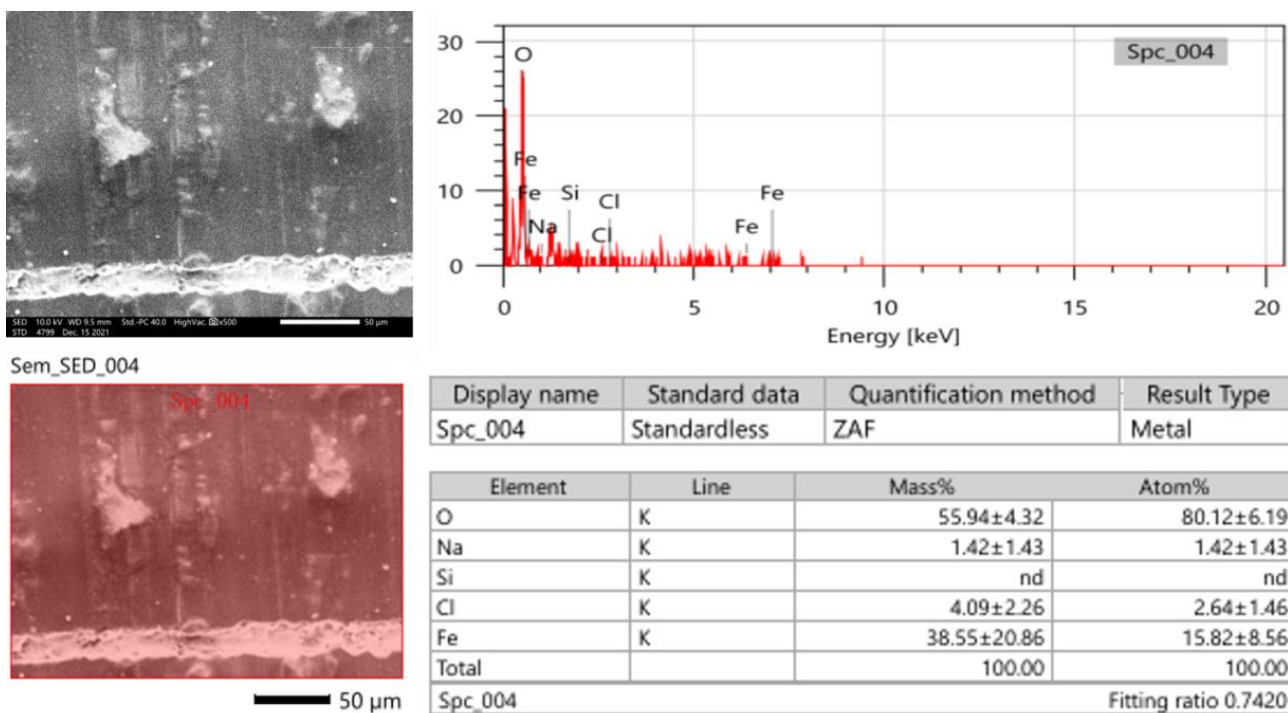


Figure 6. SEM images and EDS of 2# high induction non-oriented silicon steel after corrosion

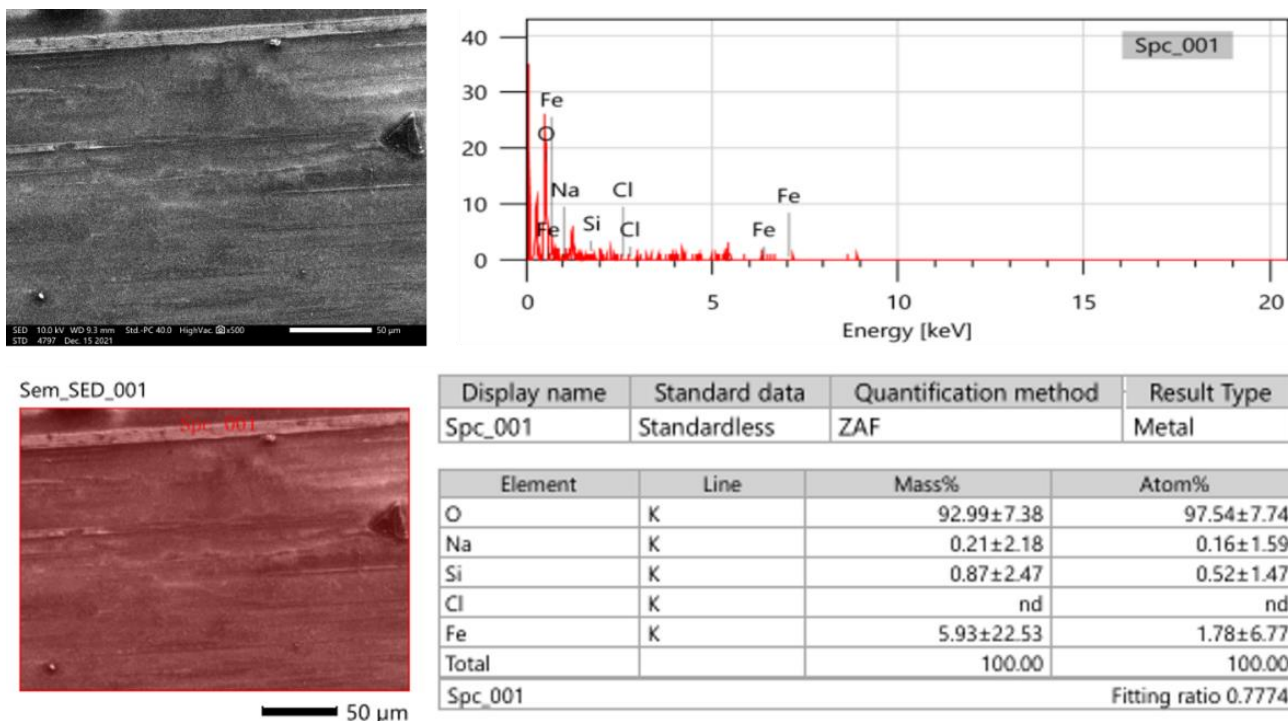


Figure 7. SEM images and EDS of 3# high grade non-oriented silicon steel after corrosion

Fig. 5, Fig. 6 and Fig. 7 are SEM images and EDS of three non-oriented silicon steels after corrosion. From the SEM morphology after corrosion, it can be seen that the surface corrosion

morphology of low grade non oriented silicon steel is the roughest, and the iron content is the highest, which is 74.64%, indicating that the corrosion is the most serious. The highest surface oxygen content of 27 is 92.99%, indicating that there is a dense oxide film on the surface. At the same time, the surface silicon content is the highest and the iron content is the lowest, indicating that the increase in silicon is conducive to the formation of a stable protective film on the surface of electrical steel under the extreme environment of wet thermal coupling and protects the alloy from further corrosion.

4. CONCLUSIONS

(1) The non-oriented silicon steel surface roughness increases with increasing Si content because of the slab microstructure heredity and hot-rolled plate with shot blasting and pickling treatment.

(2) Non-oriented silicon steel has a good self-corrosion potential and maintains such high corrosion resistance in the extreme environment of wet thermal coupling. The best high-grade non oriented silicon steel is -0.546.

(3) The highest surface oxygen content of high-grade non oriented silicon steel after corrosion is 92.99%, indicating that there is the formation of a dense oxide film on the surface. At the same time, the surface silicon content is the highest, and the iron content is the lowest, indicating that the increase in silicon is conducive to the formation of a stable protective film on the surface of non-oriented steel in the extreme environment of wet thermal coupling and protects the alloy from further corrosion.

ACKNOWLEDGMENTS

This work was supported by the Science and Technology Major Project of Shanxi Province(20191102004).

References

1. H.T. Jiao, Y.B. Xu, L.Z. Zhao, R.D.K. Misra, Y.C. Tang, M.J. Zhao, D.J. Liu, Y. Hu and M.X. Shen, *Mater. Charact.*, 156 (2019) 109876.
2. F. Fang, S.F. Che, D.W. Hou, Y.X. Zhang, Y. Wang, W.N. Zhang, G. Yuan, X.M. Zhang, R.D.K. Misra and G.D. Wang, *Mater. Sci. Eng. A*, 831 (2022) 142284.
3. Y.X. Zhang, M.F. Lan, Y. Wang, F. Fang, X. Lu, G. Yuan, R.D.K. Misra and G.D. Wang, *Mater. Charact.*, 150 (2019) 118.
4. D.S. Petrovic, *Mater. Tehnol.*, 44 (2010) 317.
5. M. Nioi, S. Celotto, H. Shimanaka, Y. ITO, K. Matsumura and B. Fukuda, *J. Magn. Magn. Mater.*, 26 (1982) 57.
6. A. Lin, X. Zhang, D.J. Fang and M. Yang, *Anti-Corros. Methods Mater.*, 57 (2010) 297.
7. Q. Ren, L.F. Zhang and W. Yang, *Steel Res. Int.*, 89 (2018) 1800047.
8. Y. Kurosaki, H. Mogi, H. Fujii, T. Kubota and M. Shiozaki, *J. Magn. Magn. Mater.*, 320 (2008) 2474.
9. L. Cheng, P. Yang, Y.P. Fang, W.M. Mao, *J. Magn. Magn. Mater.*, 324 (2012) 4068.
10. J. Xu, J. Chen, L.H. Yu, *Vacuum*, 131 (2016) 51.
11. W.X. Dou, G. Yuan, M.F. Lan, Y.X. Zhang and M. Y. Zhu, *Steel Res. Int.*, 91 (2020) 1900286.

12. W.K. Zhang, W.M. Mao, Y.D. Wang, H.F. Li and Z.H. Bai, *Iron & Steel*, 42 (2007) 64.
13. J.L. Alamilla, M.A. Espinosa-Medina, E. Sosa, *Corros. Sci.*, 51 (2009) 2628.
14. M.A. Veloz, I. Gonzalez, *Electrochim. Acta*, 48 (2002) 135.
15. V.V. Basabe, *ISIJ Int.* 57 (2017) 148.

© 2022 The Authors. Published by ESG (www.electrochemsci.org). This article is an open access article distributed under the terms and conditions of the Creative Commons Attribution license (<http://creativecommons.org/licenses/by/4.0/>).